Pergamon

Int. J. Solids Structures Vol. 35, No. 13, pp. 1451–1465, 1998

0020–7683/98 $19.00 + .00

PII: S0020–7683(97)00124–8

BUCKLING OF MULTIPLE DELAMINATED BEAMS

D. SHU
School of Mechanical and Production Engineering, Nanyang Technological University, Nanyang Avenue, Singapore 639798
E-mail: mdshu@ntu.edu.sg

(*Received* 27 *November* 1996; *in revised form* 21 *February* 1997)

Abstract—Delaminations weaken a laminated beam, which then fails prematurely under in-plane compression. An exact buckling analysis is performed for beams with double delaminations. Novel adoption of two coordinates and choice of slope as the unknown function reduce the buckling equations to simple solvable geometric equations. Complex buckling behaviors emerge for different sizes and depths of the delaminations. "Free mode" and "constrained mode" of buckling are identified. Both global and local buckling occurs, depending upon the slenderness ratios of the delaminations. In addition, an upper bound and a lower bound of buckling loads are obtained by assuming totally "constrained" and totally "free" deformation for the delaminated beam. These bounds are easy to compute and provide useful approximations. © 1998 Elsevier Science Ltd.

1. INTRODUCTION

Air entrapment or insufficient resin during fabrication of fiber-reinforced laminated composites may develop into delaminations during loading. Impact on laminated composite plates or sandwich plates also may cause delamination. These delaminations and their further extension reduce the strength of laminated composites under longitudinal compression, and can be a strength limiting factor. Such a delamination was first modeled by Chai *et al.* (1981) as a delaminated beam, wherein local delamination growth and stability were investigated. Simitses *et al.* (1985) further developed a one-dimensional model to examine the effects of delamination position, size and depth. Yin *et al.* (1986) and Kardomateas and Schmueser (1988) continued with post-buckling analysis and solved the ultimate axial load capacity of a beam with single delamination. For some geometry and fracture toughness combinations the buckling load can serve as a measure of the load-carrying capacity of the delaminated composites. Gillespie and Carlsson (1991) conducted experiments on the delamination buckling and extension on laminate composites, and verified earlier analyses. Somers *et al.* (1991), Frostig *et al.* (1992), Frostig (1992), and Frostig and Baruch (1993) extended the analysis to the local buckling of delaminated sandwich beams, with consideration of other high-order effect. Hwu and Hu (1992) further developed a one-dimensional model to analyze the global buckling of sandwich beams with debonding.

Shu and Mai (1993a) considered the bridging between delaminated laminates, which was found to delay buckling of the composites and thus has a favorable effect on their strength under longitudinal compression. Shu and Mai (1993b) examined the deformation at the two ends of the delamination, and identified "rigid connectors" and "soft connectors". Cox (1991), and Shu and Mai (1993c) showed that stitching as a form of bridging enhances the fracture resistance of laminated composite and demonstrated the multi-wave buckling configuration. Kardomateas (1993) examined the initial post-buckling and growth behavior of internal delaminations in composite plates with perturbation approximation procedure.

The above works are on one-dimensional beam-plates with single delamination. Two-dimensional plates with single delamination have mostly been numerically investigated. Yeh and Tan (1994) analyzed the buckling of elliptically delaminated composite plates with nonlinear finite element method (FEM). They used degenerated shell element and

considered large deformation. Their solution included both global and mixed modes of buckling.

In addition to the single delamination described above, multiple delaminations also may be caused by impact damages or manufacturing defects. However, little attention has been paid to the multiple delamination problem. Kapania and Wolfe (1989) used a finite element formulation to study the buckling behavior of an axially loaded beam-plate with multiple delaminations. They modeled the beam-plate with 6 degree-of-freedom beam-column elements. The possible contact between the multiple delaminated layers of the beam-plate was not considered. Lim and Parsons (1993) performed a linearized buckling analysis of a composite beam with double delaminations. They used energy method with assumed displacement and Lagrangian multipliers to account for boundary and continuity conditions. The possible contact between different layers of delamination, however, was not considered. Their analysis was also an approximate solution.

The present work seeks to accurately solve the double delamination buckling as five interconnected beams without assuming displacement. Classical beam theory is used. The solution is simplified by using two coordinates as well as the choice of slope as the unknown function. The analysis shows complicated modes of buckling depending upon the relative slenderness of the delaminated layers. Depending upon the magnitudes of the interlaminar fracture toughness, the buckling load, failure strains of the material, the delaminated beam could eventually fail in a variety of ways. The present work is restricted to the buckling-controlled strength of beams. Postbuckling deformation and delamination extension are not attempted.

2. FORMULATION

Figure 1 shows the geometry of the delaminated beam under consideration. The beam has length of L and thickness of H. The two delaminations have equal length of a and divide the beam into three layers with thickness of H_2, H_3, H_4. Consider a one-dimensional

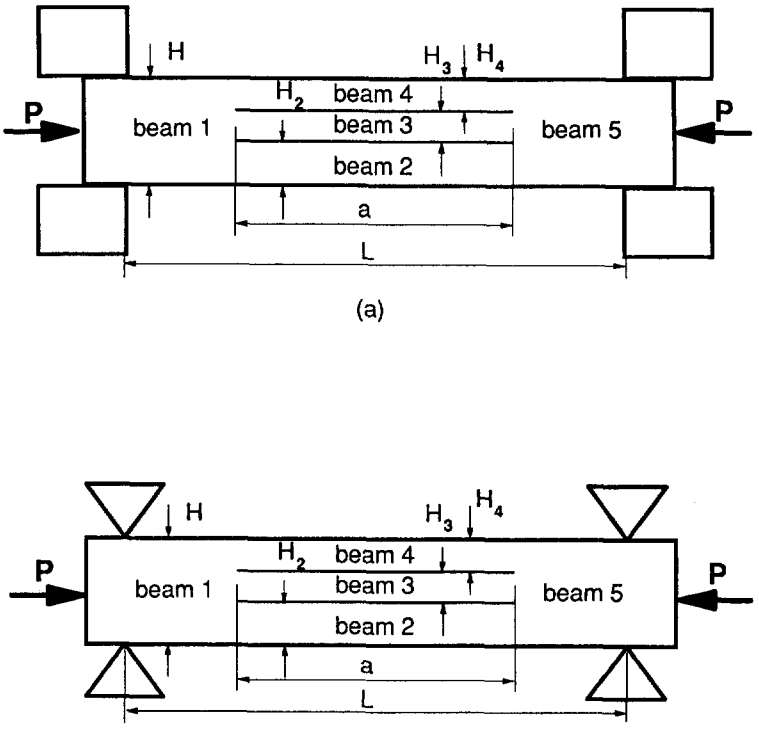

Fig. 1. A beam with double through thickness delaminations buckles under compression: (a) clamped; (b) simply-supported.

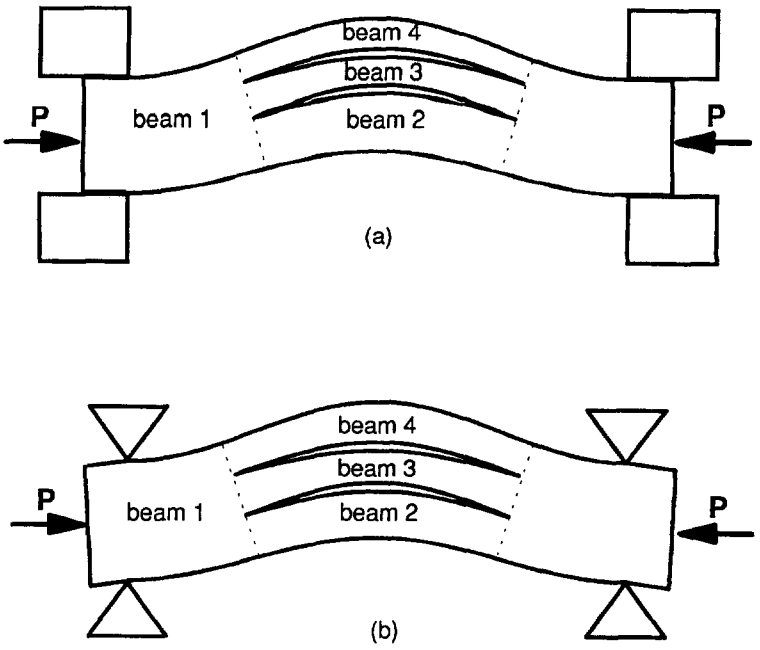

Fig. 2. Beams 2, 3 and 4 can either buckle in contact with each other, or leave gaps: (a) clamped; (b) simply-supported.

through delamination and, thus, the unit width is conveniently defined. For a two-dimensional problem, the solution is more complicated and numerical solutions would have to be sought [i.e. Narita and Leissa (1990)]. The present work is restricted to one-dimensional beams to obtain exact solutions. The delamination is located at mid-length, where it has the strongest effect (Simitses *et al.*, 1985). The beam is divided into virgin beams 1 and 5, and the delaminated beams 2, 3 and 4.

Under longitudinal compression (Fig. 2), the thinnest amongst beams 2, 3 and 4 tends to buckle first and has a higher magnitude of deformation than the thicker ones. However, the thinnest beam may be constrained by others, and they have to buckle together in a "constrained mode". This greatly complicates the problem, which has the following three types of initial buckling:

(1) "Free mode": $H_2 > H_3 > H_4$, or $H_4 > H_3 > H_2$. Without loss of generality, $H_2 > H_3 > H_4$ is chosen. In this case beams 2, 3 and 4 buckle independently of each other.

(2) "Constrained mode": $H_2 > H_4 > H_3$ or $H_4 > H_2 > H_3$. $H_2 > H_4 > H_3$ is chosen. Although the thinnest beam three buckles first, it will impinge on and be stopped by thicker beam 4 which has not yet buckled. The two later buckle together.

(3) "Partially constrained mode": $H_3 > H_2 > H_4$ or $H_3 > H_4 > H_2$. For $H_3 > H_2 > H_4$, the thinnest, beam 4, buckles freely first. Beams 2 and 3 will then follow beam 4 to buckle towards the same side (Yin *et al.*, 1986). Since beam 2 is thinner than beam 3, and thus has a larger deformation, beam 2 is constrained by beam 3. Beam 2 impinges on and is stopped by beam 3. The two beams later buckle together. The formulation of case 3 is similar to case 2 and is, thus, omitted for the sake of brevity. The above "constrained mode" and "free mode" describe the way the delaminated beam deforms, and should not be confused with the "constrained mode" and "free mode" in delamination vibration analyses [i.e. Mujumdar and Suryanarayan (1988)], where the two terms referred to approximate models. The next two sections, 2.1 and 2.2, examine cases 1 and 2, respectively, with both clamp and simple supports.

2.1. *"Free mode"*

2.1.1. *Clamped beams.* The choice of two coordinates x_1 (from left) and x (from the center) are adopted to simplify the formulation (Fig. 3). $W_i(x)$ designates the elastic and small deflection of segment i ($i = 1$ to 4). The bending moment distribution along the beams

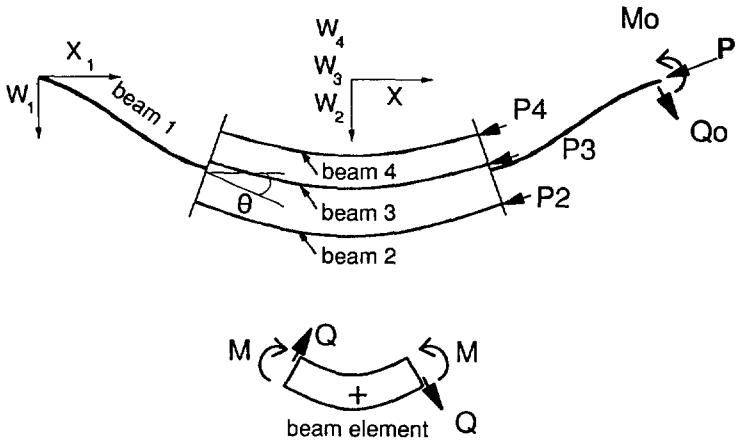

Fig. 3. The beam is modeled by five interconnected beams. Classic sign convention is adopted.

$M_i(x)$ can thus be expressed as $-EI_iW_i''(x)$. for a beam segment from one end to an internal cross-section at x (or x_1), equilibrium yields:

$$EI_iW_i''(x)+P_iW_i(x)+Q_{i0}x+M_{i0}=0, \quad (i=1\text{–}4), \tag{1}$$

where E is Young's modulus, $I_i=H_i^3/12$ is the second moment of the rectangular cross-section, Q_{i0} and M_{i0} are the shear force and bending moment at one end of the beam under consideration. Symmetry of the problem leads to zero shear at the left end of beam 1, and the center (right end) of beam 2, 3 and 4. Thus, Q_{i0} vanishes for all beams. Therefore, eqn (1) can be differentiated to yield:

$$EI_iW_i'''(x)+P_iW_i'(x)=0, \quad (i=1\text{–}4),$$

which has general solutions

$$W'(x)=S\sin(kx)+C\cos(kx), \tag{2}$$

where S and C are constants, $k^2=P/(EI)$. The choice of $W'(x)$, instead of $W(x)$ as the unknown function, simplifies the solution. For beam 1, left end clamp condition $W_1'(x_1=0)=0$ reduces the solution in eqn (2) to:

$$W_1'(x_1)=S\sin(k_1x_1). \tag{3}$$

If θ is the slope at delamination front $x_1=(L-a)/2$ (or $x=-a/2$) (Fig. 3), it follows:

$$W_1'(x_1)=-\theta\sin(k_1x_1)/\sin\left(k_1\frac{L-a}{2}\right). \tag{4}$$

Similarly, since the slope is $-\theta$ at $x=-a/2$ and zero at $x=0$ for beams 2, 3 and 4 due to symmetry:

$$W_i'(x)=\theta\sin(k_ix)/\sin\left(k_i\frac{a}{2}\right), \quad i=2,3,4, \tag{5}$$

where $k^2=k_1^2=P/EI$, $k_i^2=P_i/EI_i$, $P_i=PH_i/H$. Next, consider the moment equilibrium at the junction between beam 1, and beams 2, 3 and 4, where the bending moment in beam 1 is:

$$M_1\left(\frac{L-a}{2}\right) = -EIW_1''\left(\frac{L-a}{2}\right) = EI\theta k \cot\left(k\frac{L-a}{2}\right). \tag{6}$$

Similarly, the bending moments in beams 2, 3 and 4 are:

$$M_i\left(-\frac{a}{2}\right) = -EI_iW_i''\left(-\frac{a}{2}\right) = -EI_i\theta k_i \cot\left(k_i\frac{a}{2}\right), \quad i = 2,3,4. \tag{7}$$

The moment equilibrium about the centerline of beam 1 at the junction yields:

$$M_1 = M_2+M_3+M_4+\Delta P_2\frac{H-H_2}{2}+\Delta P_3\left(\frac{H}{2}-H_2-\frac{H_3}{2}\right)+\Delta P_4\left(\frac{H}{2}-H_2-H_3-\frac{H_4}{2}\right), \tag{8}$$

where ΔP_2, ΔP_3 and ΔP_4 are the incremental axial forces in beams 2, 3 and 4 arising from the axial extension/compression of the respective beams caused by θ (Figs 2 and 3). $\Delta P_i = P_i-(H_i/H)P$. Assuming a cross-section at the junction, $x_1 = (L-a)/2$ remains plane and perpendicular to the centerline of all beams (Fig. 2), θ would cause an extension of $\theta(H-H_2)/2$ and, thus, a strain of $\theta(H-H_2)/(2a)$ in beam 2. Therefore:

$$\Delta P_2 = EH_2\theta\frac{H-H_2}{2a}.$$

Similarly:

$$\Delta P_3 = EH_3\theta\frac{H-2H_2-H_3}{2a},$$

and

$$\Delta P_4 = EH_4\theta\frac{H-2H_2-2H_3-H_4}{2a}.$$

Substituting ΔP_2, ΔP_3 and ΔP_4 into eqn (8), it follows that:

$$E\theta\left[\begin{array}{l} Ik\cot\left(k\frac{L-a}{2}\right)+I_2k_2\cot\left(k_2\frac{a}{2}\right)+I_3k_3\cot\left(k_3\frac{a}{2}\right)+I_4k_4\cot\left(k_4\frac{a}{2}\right)+ \\ +\frac{H_2}{a}\left(\frac{H}{2}-\frac{H_2}{2}\right)^2+\frac{H_3}{a}\left(\frac{H}{2}-H_2-\frac{H_3}{2}\right)^2+\frac{H_4}{a}\left(\frac{H}{2}-H_2-H_3-\frac{H_4}{2}\right)^2 \end{array}\right] = 0. \tag{9}$$

The beam buckles when the coefficient of θ vanishes:

$$\begin{aligned} &Ik\cot\left(k\frac{L-a}{2}\right)+I_2k_2\cot\left(k_2\frac{a}{2}\right)+I_3k_3\cot\left(k_3\frac{a}{2}\right)+I_4k_4\cot\left(k_4\frac{a}{2}\right) \\ &\quad+\frac{H_2}{a}\left(\frac{H}{2}-\frac{H_2}{2}\right)^2+\frac{H_3}{a}\left(\frac{H}{2}-H_2-\frac{H_3}{2}\right)^2+\frac{H_4}{a}\left(\frac{H}{2}-H_2-H_3-\frac{H_4}{2}\right)^2 = 0. \end{aligned} \tag{10}$$

Equation (10) is nondimensionalized by

$$\frac{I_i}{I} = \left(\frac{H_i}{H}\right)^3,$$

$$\frac{k_i I_i}{kI} = \left(\frac{H_i}{H}\right)^2,$$

$$\left(k\frac{L-a}{2}\right)^2 = \frac{P}{P_c}\left(1-\frac{a}{L}\right)^2\pi^2,$$

$$(k_i a)^2 = 4\frac{P}{P_c}\pi^2\left(\frac{a}{L}\right)^2 \Big/ \left(\frac{H_i}{H}\right)^2,$$

where $i = 2, 3, 4$, and $Pc = 4\pi^2 EI/L^2$. From the resultant equation, buckling load P/Pc can be solved for different nondimensional sizes and depths of a/L and H_i/H. After the buckling load has been solved, eqns (4) and (5) can be integrated to give the buckling configurations.

2.1.2. *Simply supported beams.* Similarly, a simply-supported beam has the following slopes and buckling equation:

$$W_1'(x_1) = -\theta\cos(kx_1)/\cos\left(k\frac{L-a}{2}\right), \tag{11}$$

$$W_i'(x) = \theta\sin(k_i x)/\sin\left(k_i\frac{a}{2}\right), \quad i = 2, 3, 4, \tag{12}$$

$$-Ik\tan\left(k\frac{L-a}{2}\right)+I_2k_2\cot\left(k_2\frac{a}{2}\right)+I_3k_3\cot\left(k_3\frac{a}{2}\right)+I_4k_4\cot\left(k_4\frac{a}{2}\right)$$
$$+\frac{H_2}{a}\left(\frac{H}{2}-\frac{H_2}{2}\right)^2+\frac{H_3}{a}\left(\frac{H}{2}-H_2-\frac{H_3}{2}\right)^2+\frac{H_4}{a}\left(\frac{H}{2}-H_2-H_3-\frac{H_4}{2}\right)^2 = 0. \tag{13}$$

Equation (13) is nondimensionalized in a manner similar to eqn (10), except that the buckling load for simply-supported beam is $Pc = \pi^2 EI/L^2$.

2.2. *"Constrained mode"*

Without loss of generality, case $H_2 > H_4 > H_3$ is chosen to illustrate the "constrained mode". In this mode: (a) the delaminated beams 3 and 4 have identical transverse deformation along their entire length; and (b) frictionless sliding between them are allowed. (a) is justified because between two beams, one constraining another, the contact point will tend to spread along all their length. (b) is justified by the relative low magnitude of frictional forces compared with the axial forces in the beams. Here beams 3 and 4 buckle together as one beam, which has axial force P_3+P_4 and second moment of cross-section $I_{34} = I_3+I_4$. The resultant buckling equation for the clamped beam is:

$$-IK\tan\left(k\frac{L-a}{2}\right)+I_2k_2\cot\left(k_2\frac{a}{2}\right)+I_{34}k_{34}\cot\left(k_{34}\frac{a}{2}\right)$$
$$+\frac{H_2}{a}\left(\frac{H}{2}-\frac{H_2}{2}\right)^2+\frac{H_3}{a}\left(\frac{H}{2}-H_2-\frac{H_3}{2}\right)^2+\frac{H_4}{a}\left(\frac{H}{2}-H_2-H_3-\frac{H_4}{2}\right)^2 = 0, \tag{14}$$

where $k_{34}^2 = (P_3+P_4)/E(I_3+I_4)$. Similarly, the buckling equation for simply-supported beam is:

$$Ik\cot\left(k\frac{L-a}{2}\right)+I_2k_2\cot\left(k_2\frac{a}{2}\right)+I_{34}k_{34}\cot\left(k_{34}\frac{a}{2}\right)$$
$$+\frac{H_2}{a}\left(\frac{H}{2}-\frac{H_2}{2}\right)^2+\frac{H_3}{a}\left(\frac{H}{2}-H_2-\frac{H_3}{2}\right)^2+\frac{H_4}{a}\left(\frac{H}{2}-H_2-H_3-\frac{H_4}{2}\right)^2=0. \quad (15)$$

3. UPPER AND LOWER BOUNDS OF BUCKLING LOADS

The section only proposes to estimate the buckling load with upper and lower bounds. Delamination extension involving interlaminar fracture is not considered here. The upper bound is first considered. In general, one of beam 2, 3 and 4 tends to buckle first, and ultimate strength is reached when all beams buckle later. An upper bound can be obtained if the three are assumed to buckle simultaneously together. Constraints strengthen the delaminated beam and increase its buckling load. This simple solution avoids the tedious consideration of sequence of buckling amongst beams 2, 3 and 4, as discussed in the previous sections.

Beams 2, 3 and 4 are constrained as one beam 234, similar to beam 34 in Section 2.2. the formulation is similar to eqns (14) and (15) and is omitted. The resultant buckling equations for clamped and simply-supported beams are:

$$-Ik\tan\left(k\frac{L-a}{2}\right)+I_{234}k_{234}\cot\left(k_{234}\frac{a}{2}\right)$$
$$+\frac{H_3}{a}\left(\frac{H}{2}-\frac{H_2}{2}\right)^2+\frac{H_4}{a}\left(\frac{H}{2}-H_2-\frac{H_3}{2}\right)^2+\frac{H_4}{a}\left(\frac{H}{2}-H_2-H_3-\frac{H_4}{2}\right)^2=0. \quad (16)$$

$$Ik\cot\left(k\frac{L-a}{2}\right)+I_{234}k_{234}\cot\left(k_{234}\frac{a}{2}\right)$$
$$+\frac{H_3}{a}\left(\frac{H}{2}-\frac{H_2}{2}\right)^2+\frac{H_4}{a}\left(\frac{H}{2}-H_2-\frac{H_3}{2}\right)^2+\frac{H_4}{a}\left(\frac{H}{2}-H_2-H_3-\frac{H_4}{2}\right)^2=0, \quad (17)$$

where $I_{234}=(H_3^3+H_4^3+H_4^3)/12$, $k_{234}^2=(P_2+P_3+P_4)/E(I_2+I_3+I_4)=P/E(I_2+I_3+I_4)$.

The lower bound solution assumes that beams 2, 3 and 4 buckle freely, which ignores the interaction/constraint between them and thus reduces their buckling strength. The buckling equations are the same as eqns (10) and (13). However, in Section 2.1, eqns (10) and (13) are used with the relevant conditions of $H_2 > H_3 > H_4$. Here, in obtaining lower bound solutions, the two equations are used without preconditions.

The upper bound and lower bound formulated above are general and can be easily applied to multiple delaminations. For multiple delaminations, the conventional way to obtain exact buckling loads as in Section 2 will be very lengthy and the order of complexity will quickly render an exact solution impossible. The two bounds are, however, very easy to implement even for multiple delaminations, due to the blanket assumptions of "total free" or "total constrained". The accuracy of such approximations for a specific problem, however, needs to be further studied through either experiments or numerical schemes. The next section will include two illustrative cases.

4. RESULTS AND DISCUSSION

This section presents results obtained using the analytical model described above to study the buckling behavior of beam-plates with single and double delaminations. The present analysis is first compared with the published results on single and double delaminations. This is followed by a wide range of buckling loads and modes for double delaminations.

Table 1. Normalized buckling loads for a simply-supported beam with a single delamination, $H_2 = 0.40H$

a/L	Present solution	Lim and Parsons, (1993) energy	Lim and Parsons, (1993) Abaqus	Simitses *et al.* (1985)
0.20	0.9997	0.9997	0.9997	0.9997
0.40	0.9902	0.9902	0.9902	0.9902
0.60	0.9198	0.9198	0.9197	0.9198
0.80	0.7264	0.7264	0.7264	0.7264

To verify the accuracy of the model employed in this work, both single delamination and double delaminations were calculated using the present analysis. Table 1 shows the results from the present analysis obtained with $H_2/H = 0.4$ as the single delamination for simply-supported boundary conditions, as well as those published by Simitses *et al.* (1985), and Lim and Parsons (1993) by either FEM Abaqus or their energy method. Table 1 shows the nondimensional buckling load P/Pc, where Pc is the Euler buckling load for the undelaminated beam. $Pc = \pi^2 EI/L^2$ for simply-supported beam, and $Pc = 4\pi^2 EI/L^2$ for clamp–clamp beam. The present analysis has the same assumptions as that of Simitses *et al.* (1985) and, therefore, produces identical results. For single delamination, the contact between the two delaminated layers does not occur. Therefore, there is excellent agreement between all results. There is one exception, where the energy method of Lim and Parsons (1993), and their Abaqus FEM produced an unexpected S-shaped buckling mode shape for the lowest buckling load. The present analysis, like that of Simitses *et al.* (1985), does not produce the antisymmetric S-shaped buckling mode that is often the second mode. The energy method and Abaqus FEM introduced approximation, which might give rise to the S-shaped modes as first mode. Further work involving the numerical methods is needed to determine the exact cause of this S-shaped buckling mode shape.

To further verify the present analysis, Table 2 shows a comparison between results from the present analysis and the results generated by Abaqus and the energy method by Lim and Parsons (1993), for various lengths of double delaminations with $H_2/H = H_3/H = 0.3$ and $H_4/H = 0.4$. The agreement is excellent at short delamination length $a/L = 0.1$, and long delamination lengths $a/L = 0.4$, 0.6 and 0.8, but there are considerable discrepancies at medium lengths of $a/L = 0.2$ and 0.3, where the energy method and Abaqus FEM analysis of Lim and Parsons (1993) generated lower buckling loads than the present analysis. For all values of a/L, the buckling mode shapes from the present analysis are single-hump ones. For the energy method of Lim and Parsons (1993), the lowest buckling load mode shapes of $a/L = 0.2$, 0.3 and 0.4 are the unexpected double-hump modes, which are usually the second modes. From the present analysis, the particular geometry of $H_2/H = H_3/H = 0.3$ and $H_4/H = 0.4$ does not involve contact between buckled layers of thickness H_2 and H_3, since they have equal thickness. Although Lim and Parsons (1993) did not consider contact, this does not seem to be the reason behind the double-hump S-shaped second mode. Further investigation is needed to understand why the energy method and FEM method deviates from the present beam analysis, as well as the beam analysis by Simitses *et al.* (1985) on single delamination.

Table 2. Normalized buckling loads for a clamped beam with two delaminations, $H_2 = 0.3H$, $H_3 = 0.3H$, $H_4 = 0.4H$

Delamination length a/L	Present solution	Lim and Parsons, (1993) energy	Lim and Parsons, (1993) Abaqus
0.10	0.9996	1.000	—
0.20	0.9835	0.8939	0.8940
0.30	0.8019	0.592	—
0.40	0.5057	0.5054	0.5056
0.60	0.2374	0.2374	0.2375
0.80	0.1374	0.1374	0.1375

Comparison is also made with Kapania and Wolfe (1989), who used FEM program they developed to calculate the buckling load of double delaminations $H_2/H = H_3/H = 0.33$ for clamp–clamp boundary condition in Fig. 9 of their work. The same variation of buckling load vs delamination length a/L is obtained in Fig. 6 of the present work. The buckling loads from the present analysis are close to the buckling loads calculated by Kapania and Wolfe (1989), with the buckling loads sharply decreasing with delamination length a/L between $a/L = 0.2$ and 0.5.

In the above, results from the present analysis are verified by comparing them with either earlier results of single delamination or the energy method and FEM method on double delaminations. In the following, a wide range of nondimensional buckling loads are obtained. Since the present analysis tackles the contact between different laminates, various combinations of delamination thicknesses/depths H_2 and H_3 are investigated. This is because relative thickness between H_2 and H_3 strongly influences the contact between laminates, i.e. thinner laminates tend to buckle out more than thicker ones. Parameter $R = (a/L)/(H_4/H)$ is chosen to represent the relative slenderness of beam 4. For clamped beam (Fig. 4), $R = 1.0$ represents the case that beam 4 and the whole beam are geometrically similar. $R = 0.8$ or 1.2 represent relatively bulky or slender delamination. For simply-supported beams (Fig. 5), $Rs = (a/L)/(2H_4H)$ is chosen to represent the relative slenderness of the delaminations. To understand R and Rs, consider a so-called thin-film delamination where clamped beam 4 buckles locally. With clamped beam, local and global buckling occurs simultaneously if $R = 1$. With simply-supported beam, however, this occurs at $Rs = 1$. Beam 4 is called the surface layer and beam 3 the internal layer.

Figures 4 and 5 show the variation of normalized buckling load with surface layer thickness H_4. Figure 4 is clamped beam, while Fig. 5 for simply-supported beam. Truncation of curves $Rs = 1.2$, 1.4 in Fig. 5 are due to the physical limitation $a < L$. For both clamped and simply-supported beams, buckling load P varies with H_4 in three phases. In phase I, $H_4 < H_3$, beam 4 buckles independently first in "free mode", and R or Rs determines the almost constant P. The slight decrease of P is caused by the relatively weakened boundary constraint at the two ends of beam 4 (Fig. 2), since beam 4 is thickened in relation to the whole beam. Curves R or $Rs = 1$ have the biggest decrease in P/Pc. In transition phase II, $H_4 < H_3$, beam 3 buckles and pushes beam 4 in the "constrained mode" and thus P rapidly decreases. In phase III, the push by a thinner beam 3 is weaker and P stabilizes. For small R or Rs (0.6, 0.8, 1.0), $P = Pc$ ($P/Pc = 1$) at $a/L = 0$ (thin film buckling). For large R or Rs (1.2, 1.4), P is less than Pc due to local buckling. Take $R = 1.2$ at $a/L = 0$ in Fig. 4 as an example:

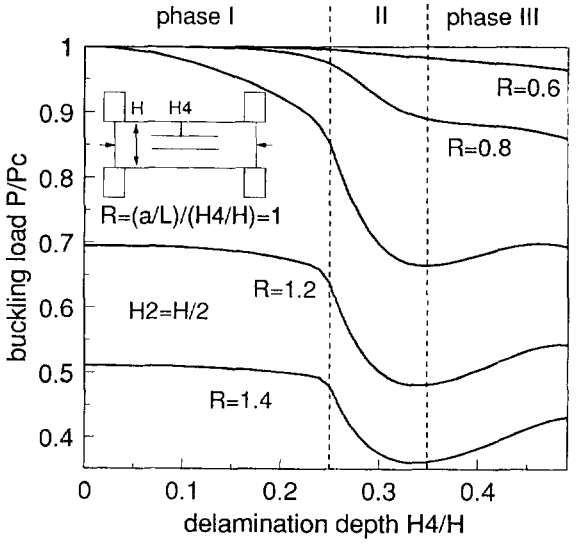

Fig. 4. The buckling load varies with delamination depth for clamp beam.

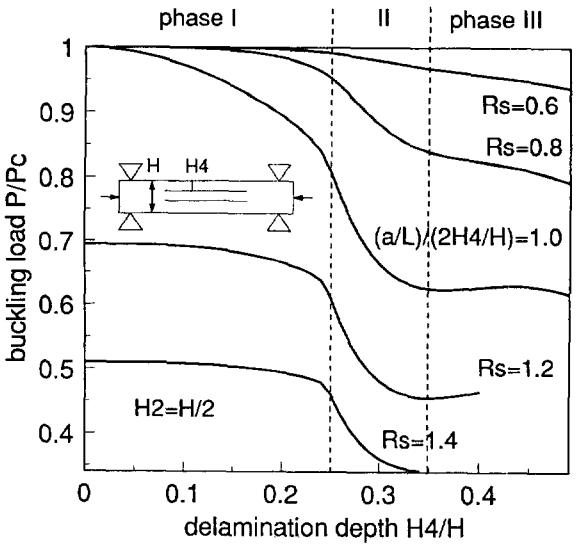

Fig. 5. $H_4 < 0.25H$ is "free mode" and $H_4 > 0.25H$ is "constrained mode".

$$\frac{P}{P_c} = \left(\frac{\pi^2 E H_4^3}{3a^2}\frac{H}{H_4}\right)\Big/\left(\frac{\pi^2 E H^3}{3L^2}\right) = \left(\frac{H_4}{H}\Big/\frac{a}{L}\right)^2 = \frac{1}{R^2} = \frac{1}{1.2^2} = 0.694,$$

where $\pi^2 E H_4^3/3a^2$ is the local buckling load of beam 4. It is worth noting that P/P_c does not vary with H_4/H monotonically. This is contrary to single delamination, where the corresponding variation is always monotonic [i.e. Yin *et al.* (1986)].

Figure 6 compares the present double delaminations analysis with earlier single delamination analysis. Single central delamination ($H_2 = H_3 = H/2$) is chosen to compare with the present double delaminations analysis. The formulation of single delamination has been done before [e.g. Chai *et al.* (1981); Simitses *et al.* (1985); Kapania and Wolfe (1989)]. Their analysis is reproduced here to calculate the buckling loads. Two cases ($H_2 = H/2$, $H_3 = H_4 = H/4$; and $H_2 = H_3 = H_4 = H/3$) of double delaminations are chosen for the present analysis. At short delamination, P is not sensitive to a. P decreases rapidly after the threshold value a/L of about 0.2. The decrease again slow at long delamination ($a > 0.5L$).

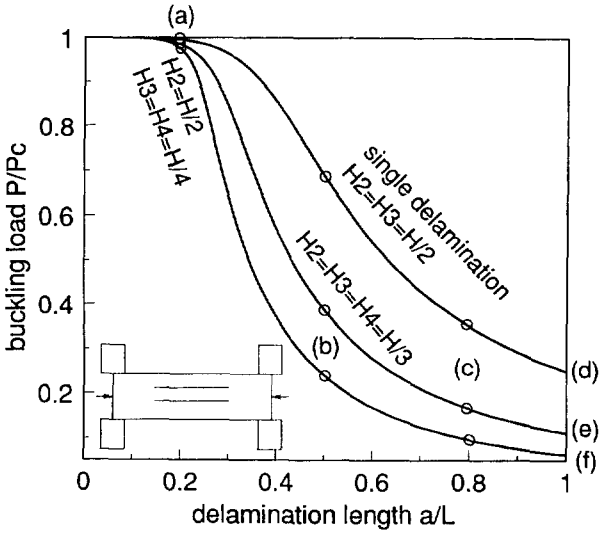

Fig. 6. Compared with single delamination, double delaminations further reduce buckling load.

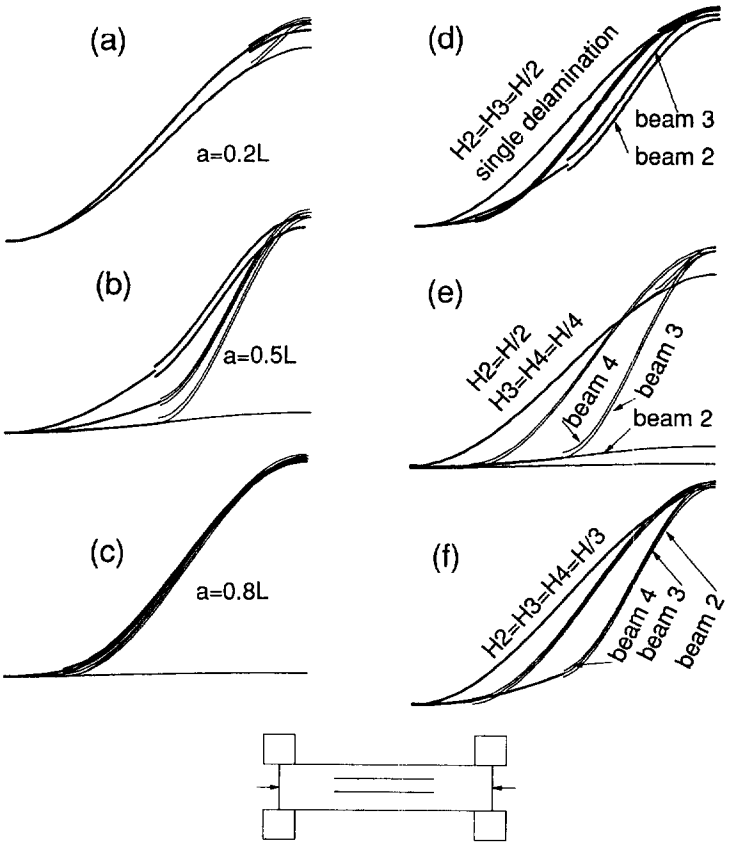

Fig. 7. the buckling configurations of clamped beams: (a) $a = 0.2L$; (b) $a = 0.5L$; (c) $a = 0.8L$; (d) $H_2 = H_3 = H/2$; (e) $H_2 = H/2$, $H_3 = H_4 = H/4$; (f) $H_2 = H_3 = H_4 = H/3$.

The buckling configurations for the circled geometries in Fig. 6 are computed and shown in Fig. 7. Figure 7(a) compares the three types of delaminations for $a = 0.2L$, while Fig. 7(b,c) for $a = 0.5L$ and $0.8L$. Figure 7(d–f) compare the same nine configurations grouped under the types of delaminations. Only half of the configurations are displayed due to symmetry. Beam 2, 3, 4 are spaced for identification although they may deform identically. The configurations are scaled to similar magnitudes to facilitate comparison. For single delamination ($H_2 = H_3 = H/2$), beam 2 and 3 buckle identically. For double delaminations $H_2 = H/2$, $H_3 = H_4 = H/4$, beam 3 and 4 buckle identically. Figure 7(b) shows the biggest difference in configuration amongst Fig. 7(a–c), corresponding to the large difference in P at $a/L = 0.5$ in Fig. 6. Thin beams 3 and 4 deform considerably more than beam 2 in Fig. 7(e), compared with identical deformation of these beams in Fig 7(d,f). Delamination portions (beams 2, 3 and 4) deform considerably more than the undeformed beam 1.

The influence of H_4 for clamped and simply-supported beams is examined in Figs 8 and 9. The buckling load P increases with H_4 in two phases. In phase I with thin surface layers, P increases rapidly. There is a kink for each of the curves at a location near $H_4 = H/4$, after which P increases relatively slowly. The reason is that for $H_4 > H/4$, $H_3 < H/4$, thus beam 4 is thicker than beam 3. Beam 3 buckles first and pushes beam 4 to buckle. The push weakens beam 4 and slows the increase of buckling load. Relative slenderness $R > 1$ for $a/L = 0.4, 0.5, 0.6, 0.8$ in Fig. 8, and $Rs > 1$ for $a/L = 0.6$ and 0.8 in Fig. 9. In both cases local buckling dominates and the kink is located at $H_4 = H/4$. For the remaining curves where R or $Rs < 1$, global buckling occurs and the kink is shifted. It is also clear that delamination affects clamped beams more than simply-supported beams.

The upper and lower bounds are computed and compared with the actual buckling load in Figs 10 and 11. The two bounds are calculated according to the analyses in Section 3, while the actual buckling load is computed according to Section 2. For $H_4 < H/4$, thus

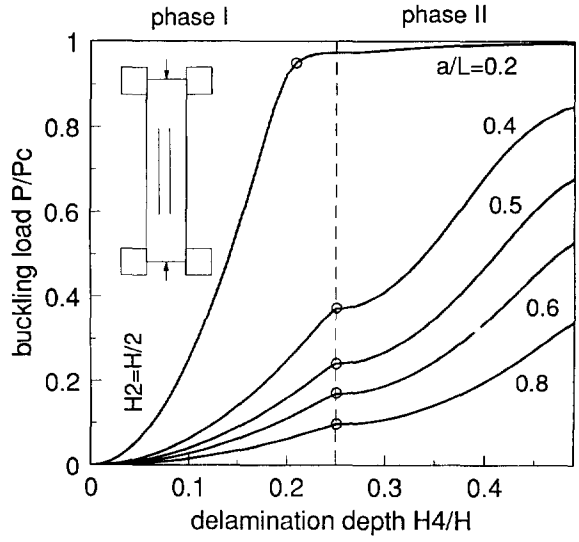

Fig. 8. Buckling load P increases with the surface delamination depth H_4 in two phases.

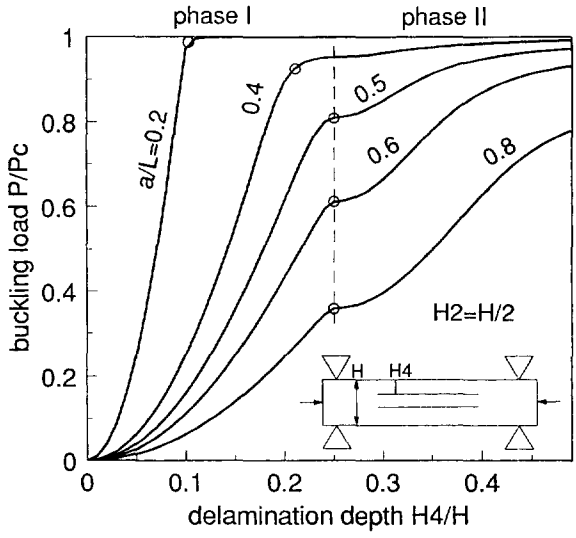

Fig. 9. Simply-supported beam is similar to clamped beam in Fig. 8.

$H_2 > H_3 > H_4$, there is no contact between layers, therefore, the lower bound equals to the actual buckling load. At $H_4 = H/2$, the internal delamination disappear and the upper bound converges unto the actual buckling load. For thick surface delamination $R = 0.8$ in Fig. 10 and $Rs = 0.8$ in Fig. 11, the upper bound is close to the actual buckling load, while for R or $Rs = 1$ and 1.2, the two diverge. In general, the upper bound provides good estimates for R or $Rs < 1$, especially for relatively thin delamination (low H_4/H). The lower bound, on the other hand, provides good approximation for shallow surface layer H_4.

The dominating influence of the slenderness ratio R on buckling load is examined for clamped beams in Fig. 12. The (H_3 H_4) couples label the crowded five curves by their order. For higher slenderness ratio R, local buckling dominates and, thus, R determines the buckling load. At low R, global buckling prevails and the influence of the delamination fades. There are two groups of curves $H_4 > H_3$ and $H_3 > H_4$, where curves in group $H_3 > H_4$ represent "free mode" of buckling, while curves in group $H_4 > H_3$ represent "constrained mode" of buckling. The two groups of curves corroborate the two phases in Figs 8 and 9, where phase I ("free mode") and phase II ("constrained mode") have different characteristics. The buckling of simply-supported beams is similarly influenced by slenderness ratios Rs. It is possible to obtain good approximation of buckling load for high slenderness

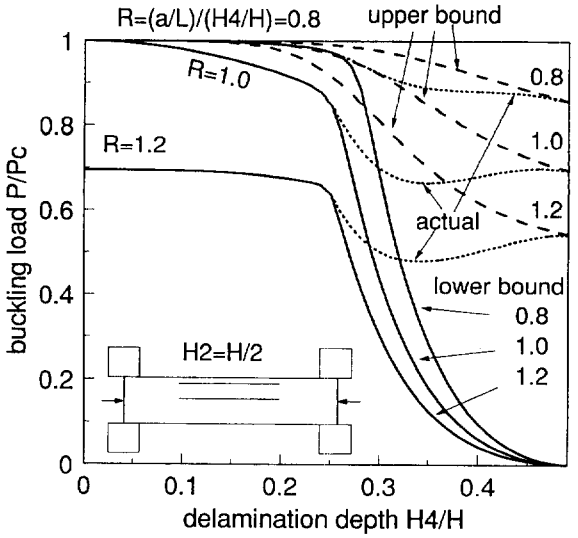

Fig. 10. Upper bound and lower boundary compared with actual buckling load for clamped beam.

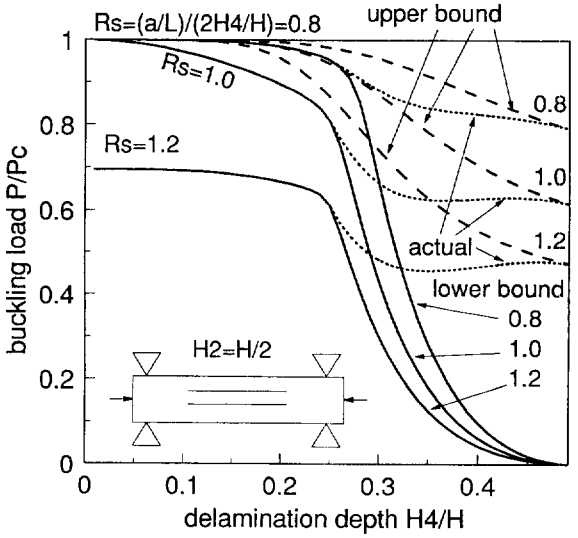

Fig. 11. Upper bound and lower bound for simply-supported beam.

ratio ($R > 1.2$) from Fig. 12. Since the curves in one of the two groups in Fig. 12 are close to each other. Buckling load can be assumed to depend on slenderness ratio only within each group. It is worth noting, however, that the dependence is different for the two groups.

Post-buckling deformation and delamination extension are not analyzed here. Those analyses are complex and, thus, deserve their own separate treatment [i.e. Shu and Mai (1993c)]. Thus, the present analysis is restricted to the class of problem of high fracture toughness and where the compressive strength of the beam is determined by buckling rather than delamination extension. The buckling configurations obtained, however, can aid the analysis of post-buckling as well as delamination extension. Apart from being the solution of a basic delamination buckling problem, the solution can also serve as a benchmark test case for other general numerical/approximation schemes for multiple delamination buckling problem.

5. CONCLUSIONS

An exact solution of the buckling of double delaminated beams is obtained for the first time. The beam is found to buckle either together in "constrained mode", or independently in "free mode", or in mixed "partially constrained mode", depending upon the

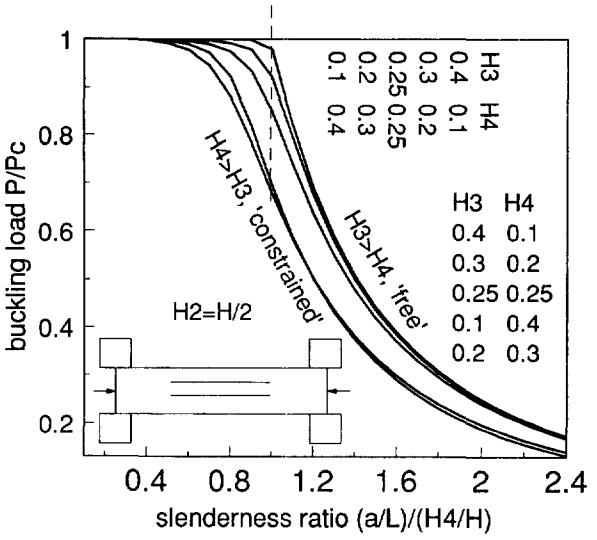

Fig. 12. Slenderness ratio R dominates the buckling load for both "constrained" and "free mode".

relative thickness of the delaminated layers of the beam. The sensitivity of buckling load towards either the depth or the length of the delamination increases quickly after some threshold values of either the depth or the length. The slenderness ratios defined are found to dominate the buckling loads of the delaminated beams. However, the dominance for "constrained mode" is different from that for "free mode". Simple ways to calculate upper bounds and lower bounds of the buckling loads are proposed, which render useful approximations especially for multiple delaminations.

Acknowledgement—The author wishes to thank the Applied Research Fund for the continuing support of this work which forms part of the program on "Stitching and vibration in composite delamination", under the grant RG52/94.

REFERENCES

Chai, H., Babcock, C. D. and Knauss, W. G. (1981) One dimensional modelling of failure in laminated plates by delamination buckling. *International Journal of Solids and Structures* **17**(11), 1069–1083.

Cox, B. N. (1991) Fundamental concepts in the suppression of delamination buckling by stitching. *Ninth DoD-/NASA/FAA Conference of Fibrous Composites in Structural Design*, Lake Tahoe, Nevada, pp. 1105–1110.

Frostig, Y. (1992) Behavior of delaminated beam with transversely flexible core—high-order theory. *Composite Structures* **20**, 1–16.

Frostig, Y. and Baruch, M. (1993) High-order buckling analysis of sandwich beams with transversely flexible core. *Journal of Engineering Mechanics, ASCE* **119**(3), 475–495.

Frostig, Y., Baruch, M., Vilnay, O. and Sheinman, I. (1992) High-order theory for sandwich-beam behavior with transversely flexible core. *Journal of Engineering Mechanics, ASCE* **118**, 1026–1043.

Gillespie, J. W., Jr and Carlsson, L. A. (1991) Buckling and growth of delamination in thermoset and thermoplastic composites. *Journal of Engineering Materials and Technology* **113**(1), 93–98.

Hwu, C. and Hu, J. S. (1992) Buckling and postbuckling of delaminated composite sandwich beams. *AIAA Journal* **30**, 1901–1908.

Kapania, R. K. and Wolfe, D. R. (1989) Buckling of axially loaded beam-plate with multiple delaminations. *Journal of Pressure Vessel Technology* **111**, 151–158.

Kardomateas, G. A. (1993) Ultimate axial load capacity of a delaminated beam-plate. *Journal of Applied Mechanics* **60**(4), 903–910.

Kardomateas, G. A. and Schmuester, D. W. (1988) Buckling and postbuckling of delaminated composites under compressive loads including transverse shear effects. *AIAA Journal* **26**, 337–343.

Lim, Y. B. and Parsons, I. D. (1993) Linearized buckling analysis of a composite beam with multiple delaminations. *International Journal of Solids and Structures* **30**(22), 3085–3099.

Mujumdar, P. M. and Suryanarayan, S. (1988) flexural vibrations of beams with delaminations. *Journal of Sound and Vibration* **125**(3), 441–461.

Narita, Y. and Leissa, A. W. (1990) Buckling studies for simply-supported symmetrically laminated rectangular plates. *International Journal of Mechanical Science* **32**(11), 909–924.

Shu, D. and Mai, Y.-W. (1993a) Delamination buckling with bridging. *Composite Science and Technology* **47**, 25–33.

Shu, D. and Mai, Y.-W. (1993b) Buckling of delaminated composites re-examined. *Composite Science and Technology* **47**, 35–41.

Shu, D. and Mai, Y.-W. (1993c) Effect of stitching on interlaminar delamination extension in composite laminates. *Composite Science and Technology* **49,** 165–171.

Simitses, G. J., Sallam, S. and Yin, W. L. (1985) Effect of delamination of axially loaded homogeneous laminated plates. *AIAA Journal* **23**(9), 1437–1444.

Somers, M., Weller, T. and Abramovich H. (1991) Influence of predetermined delaminations on buckling and postbuckling of composite sandwich beams. *Composite Structures* **17,** 295–329.

Yeh, Meng-Kao and Tan, Chung-Ming (1994) Buckling of elliptically delaminated composites plates. *Journal of Composite Materials* **28**(1), 36–52.

Yin, W. L., Sallam, S. N. and Simitses, G. J. (1986) Ultimate axial load capacity of a delaminated beam-plate. *AIAA Journal* **24**(1), 123–128.